IJE TRANSACTIONS B: Applications Vol. 35, No. 08, (August 2022) 1501-1508

International Journal of Engineering

Journal Homepage: www.ije.ir

Effect of Active Flux on Aluminum 6061 and its Mechanical Properties by Gas Tungsten Arc Welding Process

R. Ajezi-Sardroud[a], A. Mostafapour[a], F. Ajezi-Sardroud*[b], M. A. Mohtadi-Bonab[b]

[a] *Department of Mechanical Engineering, University of Tabriz, Tabriz, Iran*
[b] *Department of Mechanical Engineering, University of Bonab, Bonab, Iran*

PAPER INFO

Paper history:
Received 16 Febraury 2022
Received in revised form 16 March 2022
Accepted 19 March 2022

Keywords:
Tungsten Inert gas
Aluminum Alloy
Mechanical Properties
Active Flux
Titanium Oxide
Silicon Oxide

ABSTRACT

The current research was carried out with the aim of increasing the penetration depth and improving the mechanical properties of weld region by addition of active fluxes of titanium oxide (TiO_2) and silicon oxide (SiO_2). Tungsten inert gas (TIG) welding is applied on Aluminum 6061 alloy and active fluxes including SiO_2 and TiO_2 with 2.5, 7.5, and 10 wt% were incorporated. Up to now, TIG welding on aluminum 6061 with SiO_2 and TiO_2 fluxes has not been carried out. Mechanical properties were determined using tensile and Vickers micro-hardness experiments. The results showed that the highest tensile strength corresponds to the base metal and in welded specimens was related to 10% TiO_2 active flux. The ratio of tensile strength using titanium active flux and without flux mode is 90%. The use of both active titanium oxide and silicon oxide flux make the welded specimen granular and increases its strength. The effect of addition of titanium oxide is more noticeable than that of the silicon oxide flux since titanium oxide plays a key role on the granularity than the silicon oxide.

***doi**: 10.5829/ije.2022.35.08b.06*

1. INTRODUCTION

Aluminum 6061 has a great weldability feature in which thin parts are welded by tungsten arc welding technique while thick parts are welded by electric arc welding method [1]. The strength of this alloy is reduced after the welding process [2]. In 1920's, a great effort was designated to improve the quality of welding using arc protection and molten puddle in front of the atmosphere. One of the most important methods is the use of active flux in TIG welding process, which is known as active TIG. Tungsten is a hard metal with a melting point temperature of about 3800 °C [3]. The base metal molten puddle is protected from atmospheric elements by inert gas especially against combining with oxygen since inert gas does not mix with any of affinity elements. As soon as, the inert gas flows, the oxygen and air in the welding zone are pushed aside [4]. The protective gas passes through the tungsten electrode by a torch which is partly effective for cooling of the tungsten. Inert gas is mostly argon, but helium and nitrogen are also used in some cases depending on the type of application. The helium is used since it causes an increase in arc power and due to this, the speed of welding can be raised. This phenomenon also causes a better gas emissions from the weld zone [5]. It is worth mentioning that AC and DC currents are used in TIG welding [6]. Since welding rate in TIG method is relatively low, such method is used in welding of thick sheets for welding first pass (root pass). The welding cost is inversely proportional with welding time [7]. Kulkarni et al. [8] used P91 and P22 steel plates of 8 mm thickness, activating fluxes and TIG welding method. In their study, the effect of various fluxes such as silicon dioxide, titanium dioxide, chromium oxide, molybdenum oxide and copper oxide on the weld bead shape were investigated. Ramkumar et al. [9] studied the ferritic stainless steel (AISI 430) ability of welding using with and without activating fluxes. Two types of fluxes such as silicon dioxide and iron oxide have been used for analyzing mechanical properties of weld beads of

*Corresponding Author Email: razzaghajezi@gmail.com (F. Ajezi-Sardroud)

Please cite this article as: R. Ajezi-Sardroud, A. Mostafapour, F. Ajezi-Sardroud, M. A. Mohtadi-Bonab, Effect of Active Flux on Aluminum 6061 and its Mechanical Properties by Gas Tungsten Arc Welding Process, ***International Journal of Engineering, Transactions B: Applications***, Vol. 35, No. 08, (2022) 1501-1508

AISI430. The studies showed the existence of two kinds of phase structures including ferrite-intergranular martensite and precipitate-free zone surrounding the grain boundary martensite. Venukumar et al. [10] studied the welding parameters on inconel 718 alloy welded by TIG welding method. The post-world heat treatment performed at 750°C/8h furnace and the cooling rate was at 650°C/8h/air on weld beads. The results showed that welded specimens had better mechanical properties. In another study, Ramkumar et al. [11] investigated the effect of heat treatment on microstructure and mechanical properties in inconel 750 at fusion zone welded by A-TIG method. The tensile strength in post weld heat treated was higher than the as-weld condition, while the toughness value of as-weld specimens was higher than post weld heat treated specimen. Babbar et al. [12] studied TIG welding on different thicknesses of SS-304 steel. According to results, the welded specimens had higher tensile strength. Xie et al. [13] carried out a process using AZ31 magnesium alloy as base metal, Nano particles strengthening activating flux tungsten inert gas (NSA-TIG) as welding method and compound of titanium dioxide and nano-silicon carbide as coating fluxes. The results showed that compound of nano-particles as coating activating fluxes increased the microhardness in fusion zone and tensile strength of the joints. Ezazi et al. [14] have carried out research on two types of materials named stainless steel 3041 and aluminum alloy 5083. In their study, different activating fluxes were used such as titanium dioxide and calcium fluoride. The results showed that calcium fluoride increased strength more than titanium dioxide. Khoshroyan and Darvazi [15] conducted a research on distribution of heat and residual stress in Illinois aluminum 6061-T6 by ANSYS software in which MIG welding method was applied. In this study, the fluxes were not used and the affecting factors were only speed and currents of welding. Pk et al. [16] concentrated on improving the mechanical properties of aluminum 6061-SiC composite welded by TIG method. Also, in this research, the fluxes were homogenized and aged at 100, 150 and 200°C. The results showed that the aged and homogenized specimen in laboratory conditions had optimal hardness and minimum tensile strength.

The activated TIG can increase productivity by using TiO_2 and SiO_2 fluxes. It has been reported that activating fluxes such as TiO_2 and SiO_2 increased the maximum weld penetration [17]. However, an increase in the mechanisms of penetration in the activated flux TIG welding process is not fully understood [18]. It is worth-mentioning that two mechanisms can be considered on the activating flux on weld penetration. The first one is the arc constriction in which the activating flux may induce arc constriction during TIG welding [19, 20]. In this mechanism, the heat density has increased by the activating flux at the anode root area. As a result, the activating flux increases the penetration depth. The second mechanism is the reversal of surface tension gradient showing that surface active elements including sulfur and oxygen decomposed from the flux during welding change the fluid flow direction in the weld pool [21]. The purpose of this research in gas tungsten arc welding (GTAW) was to use active flux to increase the penetration depth and improve mechanical properties of weld region. It is expected that the use of active flux in TIG welding increases the weld depth and D/w. Also, active flux causes granularity in the weld zone leading to increase of tensile strength and microhardness. For the first time in this study, Al 6061 as a base metal and SiO_2 and TiO_2 as active fluxes were used and investigated.

2. EXPERIMENTAL PROCEDURE

The primary material used in this article is aluminum 6061-T6. Chemical composition of the used metal (for GTAW process) is summarized in Table 1. For specimen preparation, first a sheet with the thickness of 6 mm of the alloy was cut with dimensions of 100 mm x 50 mm by wire cut.

The active flux powders of TiO_2 and SiO_2 powders are used in this study. In aluminum welding by activating flux, first, the specimen is covered with a thin layer of TiO_2 or SiO_2 which is mixed with acetone. For this purpose, first, the specimens are weighted and then two pieces are stuck with the glue tape with the distance of 1 cm. After weighting, each specimen is covered with related oxide.

The schematic of active flux application is shown in Figure 1. The TIG welding machine used in this study had an automatic steady-speed with the speed of 15 mm/min. The specimens were fixed by a clamp and the electricity arc was determined by a filler with 2 mm thickness.

After welding process, the apparent quality of all welded specimens was evaluated. The apparent quality of the welded specimens like excessive reinforcement, under cut and spatter were evaluated and from each of the welded specimens, one with the best quality was chosen, see Figure 2. According to Figure 2, specimens of AL6061 were welded by two different types of active

TABLE 1. Chemical composition of aluminum 6061-T6 alloy (%) [22]

Al 6061-T6	Al	Si	Mn	Mg	Cr	Zn	Ti	Cu
----	Balance	0.68	0.32	0.85	0.06	0.07	0.05	0.22

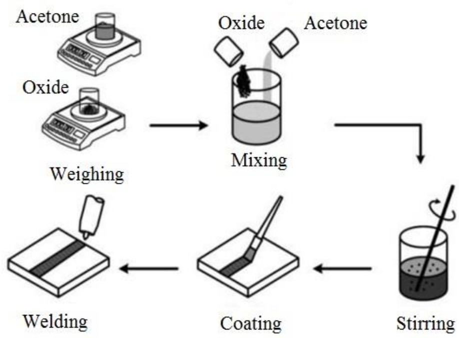

Figure 1. Schematic view of the flux application on specimens [23]

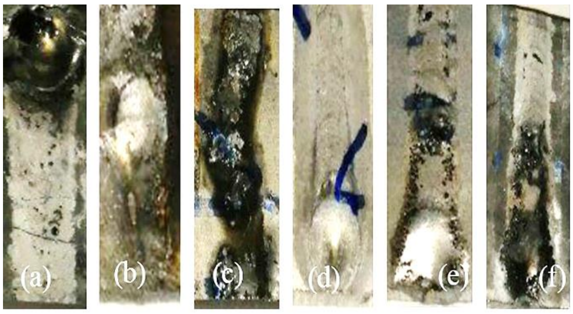

Figure 2. Physical appearance of welded specimens by (a) SiO_2 2.5% (b) SiO_2 7.5% (c) SiO_2 10% (d) TiO_2 2.5% (e) TiO_2 7.5% and (f) TiO2 10%

fluxes with different percentages of 2.5 and 7.5 and 10. Then, as shown in Figure 3, the specimens were subjected to the tensile testing.

According to Figure 4, tensile testes specimens were cut by the JIS Z2201 standard [24]. They were cut by wire cut in order to weld on their center. The specimens were under tensile test with 10 mm/min in order to examine their tensile strength and flexibility.

Vickers micro hardness testing was carried out with 200 g weight for 27 s. These 15 micro hardness experiments were carried out on each specimen which covered and evaluated the whole welding zone including the base metal, HAZ zone and weld pool.

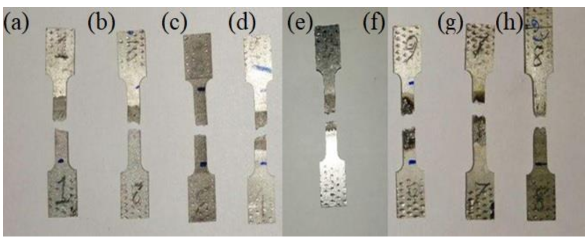

Figure 3. Tensile and micro hardness tested specimens welded by (a) without flux (b) SiO_2 2.5% (c) SiO_2 7.5% (d) SiO_2 10% (e) TiO_2 2.5% (f) TiO_2 7.5% (g) TiO_2 10% and (h) raw specimen

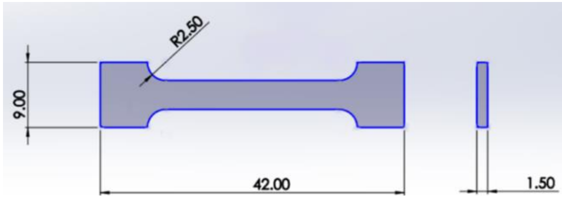

Figure 4. Dimensions of tensile tested specimens based on JIS Z2201 standard [24]

3. RESULTS AND DISCUSSION

The results of the depth-to-width ratio (D/W) measurement in welded specimens are shown in Table 2. As seen in this table, at the same inlet heat, the ratio of depth to weld width increases with increasing the percentage of activating fluxes. The reason for the increase in penetration depth is the reverse of the Marangoni flow rate of the weld pool. As is clear, elements such as oxygen, which have a high surface activity, reverse the direction of the Marangoni force and increase the depth. On the other hand, in the active mode of active flux, by decomposing the welding flux, oxygen gas escapes from the welding site and surrounds the arc. The presence of this gas prevents heat loss and narrows the arc, which ultimately increases the intensity of the flow and weld depth. As a result of the application of activating fluxes on the welding of specimens, the results show the high positive effects of surface activator flux on the depth-to-width ratio in the present study. As mentioned earlier, the main reason for the increase in penetration depth is the reversal of Marangoni displacement of the weld pool fluid, which is possible despite the elements with high surface activity [25]. The next factor affecting the depth of penetration of the weld is the increase of the temperature of the arc plasma due to the decomposition and even evaporation of the surface activating flux. By decomposing the active flux elements, the oxide molecules join the free electron ring around the arc and surround the arc [26]. The presence of this cloud layer of oxide elements around the arc prevents heat loss and arc contraction and increases the plasma flow density as well [27, 28]

The results of the ratio of depth to weld width are presented in Figure 5 and Table 2 with TiO_2 and SiO_2 active fluxes with different percentages of 2.5%, 7.5% and 10%. The results show that the ratio of depth to weld width increases with the increase of active flux. As seen in 10% of TiO_2 specimen, the highest ratio is 0.92 which is 2.68 times higher than the non-flux welded specimen.

Microstructure of specimens tested by metallographic method are shown in Figures 6(a)-6(h) and also crystal grain sizes are presented in Table 3. As seen in this figure, the application of their active flux increases the nucleation centers and, as a result, causes the smelting area to shrink

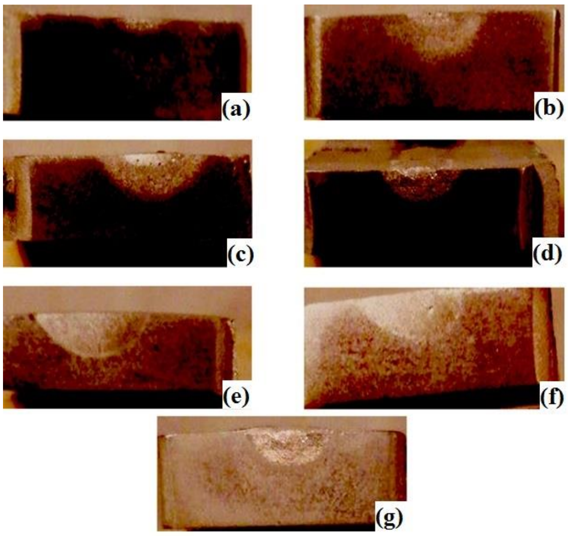

Figure 5. Penetration depth of welded specimens (a) welded without flux, (b) SiO_2 2.5%, (c) SiO_2 7.5%, (d) SiO_2 10%, (e) TiO_2 2.5%, (f) TiO_2 7.5%, and (g) TiO_2 10%

TABLE 2. Depth to width ratio of welded specimens

Specimen No.	Name	Width (W)	Depth (D)	Ratio of (D/W)
1	Welded Without Flux	6	1.5	0.25
2	SiO_2 2.5%	6	2	0.33
3	SiO_2 7.5%	6	3.5	0.58
4	SiO_2 10%	5	3	0.6
5	TiO_2 2.5%	8	6	0.75
6	TiO_2 7.5%	5	4	0.8
7	TiO_2 10%	7	6.5	0.92

[29, 30]. There are some sediments shown in the images in which the source of these sediments is the evaporation of magnesium oxide which is visible among sediments by black dots called inclusion. Figures 6(a) and 6(b) show the microstructure of raw material and welded without flux. In the raw material, there is no inclusion and precipitate; however, there are few precipitates and inclusions in welded material without flux. The precipitates and inclusions are shown with black spots. Moreover, many elongated grains are observed in both figures. Figures 6(c)-6(e) show the HAZ zone microstructures of welded specimens by adding SiO_2 2.5%, SiO_2 7.5%, and SiO_2 10%, respectively. As clearly, one can see that there are many black spots in these specimens showing that the density of precipitates and inclusions are increased with the SiO_2 addition. One can also see the elongated grains in these figures show that full recrystallization was not achieved in these grains. Figures 6(f)-6(h) show HAZ zone microstructures of welded specimens by addition of TiO_2 2.5%, TiO_2 7.5%, and TiO_2 10%, respectively. In these figures, the size of black spots is significantly increased and some subgrains are formed during welding process. More importantly, when the amount of TiO_2 increased, some big cracks are formed in the HAZ zone. As stated in Table 3, the decrease in grain size improves the mechanical properties.

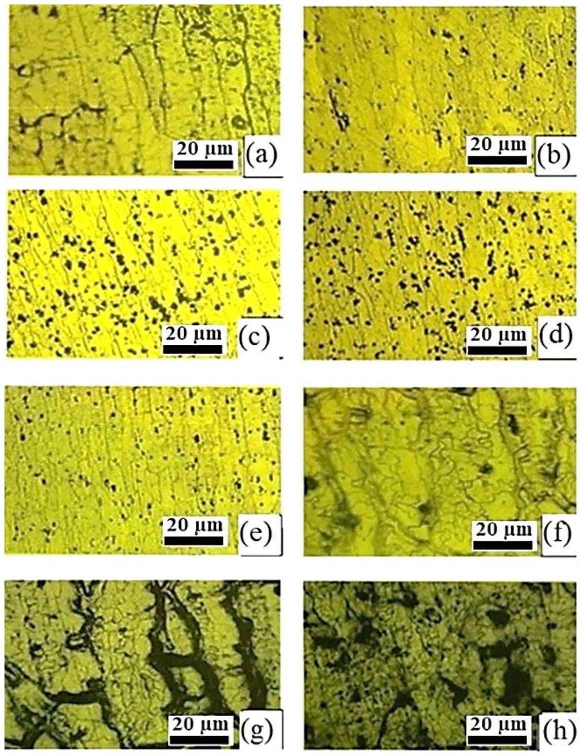

Figure 6. HAZ zone microstructures of welded specimens in 100x (a) raw material (b) welded without flux (c) SiO_2 2.5% (d) SiO_2 7.5% (e) SiO_2 10% (f) TiO_2 2.5% (g) TiO_2 7.5%, and (h) TiO_2 10%

According to Table 4, it is observed that the active flux of SiO_2 and TiO_2 is active based on the ratio of Hall-Petch and finer than active granulation without flux.

TABLE 3. Crystal grain medium sizes

Specimen No.	Name	Average grain size (µm)
1	Welded Without Flux	26
2	SiO_2 2.5%	20
3	SiO_2 7.5%	15
4	SiO_2 10%	13
5	TiO_2 2.5%	16
6	TiO_2 7.5%	14
7	TiO_2 10%	10
8	Raw specimen	23

TABLE 4. Average value of Vickers micro hardness of specimens

Specimen No.	Name	Vickers Micro Hardness (HV)
1	Welded Without Flux	66±2
2	SiO_2 2.5%	70±1
3	SiO_2 7.5%	77±3
4	SiO_2 10%	87±2
5	TiO_2 2.5%	68±2
6	TiO_2 7.5%	72±1
7	TiO_2 10%	96±3
8	Raw specimen	106±3

Therefore, the hardness of activated flux welds is higher than that of without active flux [31].

As shown in Figures 7(a) and 7(b), as the concentration of active flux increases, the melted area becomes finer which increases the hardness. The base metal, due to rolling process, increases its stiffness and hardness called work-hardening creating a cast-like structure during welding. Molten metal loses its hardening properties and due to recrystallization, the hardness of the welded parts decreases.

The results of the tensile test are summarized in Table 5. In all welded specimens, there is a correlation between the maximum elongation and the tensile strength. It is worth-mentioning that the raw specimen has the highest tensile strength and maximum elongation. A comparison with welded specimens by A-TIG method shows that the active fluxes percentage has a considerable effect on the tensile strength and strain of the tested specimen. Finer the microstructure, the better mechanical properties are achieved. For this reason, the tensile strength in specimen 7 is the highest.

By comparing the tensile test results of the specimens in Figures 8(a)-8(h), it is concluded that active flux welding has a more tensile strength than active flax-free welding. However, in the welded active flux, the welding is divided into two groups with active SiO_2 and TiO_2. In SiO_2, specimen 4 has the maximum tensile strength, including 10% SiO_2. In TiO_2, specimen 7 has the maximum tensile strength including 10% TiO_2. This indicates that in both types of activated fluxes, the tensile strength increases with increasing flux percentage. However, in general, addition of TiO_2 has achieved better results than that of the SiO_2.

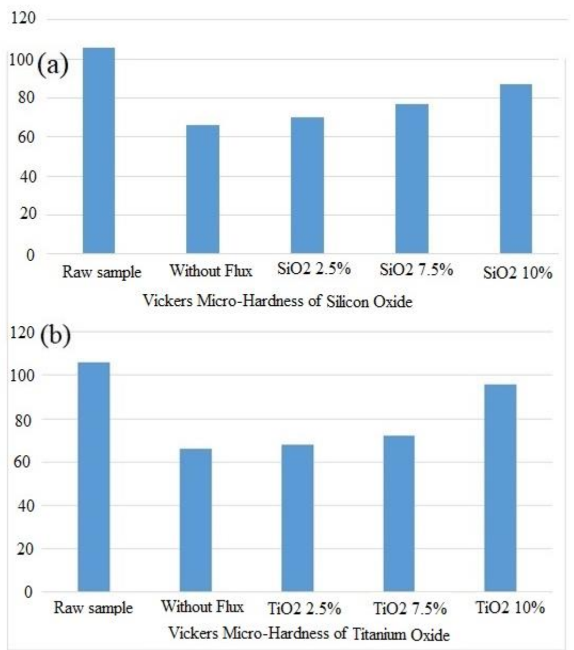

Figure 7. Vickers micro hardness of (a) SiO_2 and (b) TiO_2

TABLE 5. Tensile strength and Strain of welded specimens

Specimen No.	Name	Tensile Strength (MPa)	Max. Elongation (%)	Elasticity Modulus (GPa)
1	Welded Without Flux	80±5	3	90.2±2
2	SiO_2 2.5%	126±6	6	79.7±2
3	SiO_2 7.5%	129±4	6	83.1±3
4	SiO_2 10%	138+4	4	120.9±4
5	TiO_2 2.5%	137±6	16	43.8±2
6	TiO_2 7.5%	144±5	12	63.1±4
7	TiO_2 10%	152±5	5	100.4±3
8	Raw specimen	274±6	8	151.5 ±4

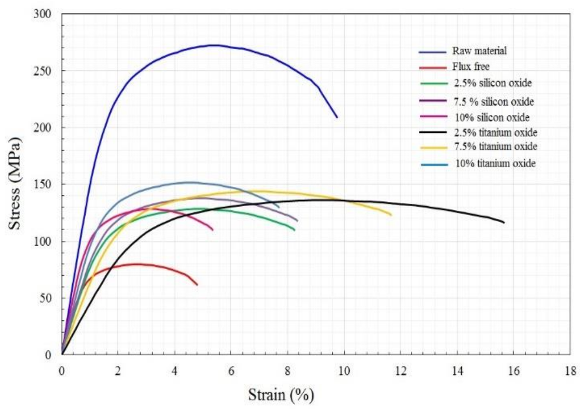

Figure 8. Stress- strain curve for (a) raw material (b) flux-free welded specimen (c) 2.5% SiO_2 active flux welded specimen, (d) 7.5% SiO_2 active flux welded specimen, (e) 10% SiO_2 active flux welded specimen, (f) 2.5% TiO_2 active flux welded specimen, (g) 7.5% TiO_2 active flux welded specimen, (h) 10% TiO_2 active flux welded specimen

Due to its eutectic state, silicon and aluminum reduce the melting temperature and an increase in the speed of melting operations and welding at the same time. In addition, all the components of silicon and aluminum melt in the solution and simultaneously begin to crystallize, which reduces stress when the welding area cools [32]. Silicon improves welding operations and reduces the percentage of gas absorption and facilitates shell freezing. Due to the reduction of the melting point and the decrease in the percentage of contraction during freezing of the weld zone, silicon has caused this to be a factor in reducing the stress when the melt area cools. The active SiO_2 flux during Al 6061 is not sensitive to hot cracking and scattered shrinkage welding due to its eutectic properties [33]. In comparison, titanium causes granularity and has a special effect on nucleation, granulation, oxidation and quality of the operations. As mentioned earlier, the reason for the granularity in the active titanium flux is its acting as non-uniform cores in freezing. Moreover, an increase in the number of cores causes the crystal lattice of the weld zone to become smaller and more uniform. Titanium makes the weld region granular, which is due to an increase in grain boundary length and strength. On the other hand, this granularity increases the flexibility. Granularity also prevents large shrinkage cavities in the weld region increasing the quality of the weld. Using active flux, no matter what type they are, both of them create granularity in the base weld metal. These active fluxes decompose due to welding heat and release oxygen. Some of oxygen atoms emit gas around the plasma channel and prevent the plasma channel from expanding. However, the narrowing of the plasma canal reduces the width of the weld and increases the depth. Also, the presence of oxygen in the melt changes the shape of the metal impurities in the composition of the elements. This phenomenon acts as granulation centers and the welding metal becomes finer. In comparison of SiO_2 and TiO_2, the presence of titanium and its oxide in the melt increases the nuclearization centers and the weld metal becomes finer. More importantly, titanium and TiO_2 nucleation role is higher than silicon and SiO_2.

Figures 9(a)-9(d) show SEM images of fracture surfaces for tensile tested specimens. As shown in Figures 9(a) and 9(b), in the fracture surfaces of raw and flux-free welded specimens, there are a lot of dimples which are considered a sign of ductile fracture. Figures 9(c)-9(e) also show the fracture surfaces of 2.5% and 7.5% and 10% SiO_2 active flux welded specimens. One can clearly see that the type of fracture is ductile due to the presence of many dimples in the fracture surfaces of these specimens. Interestingly, the fracture surface of 2.5% TiO_2 active flux welded specimen show that when TiO_2 is added to the weld part, the number of dimples is significantly reduced and the surface becomes flat. The flat surface proves that the nature of fracture transfers

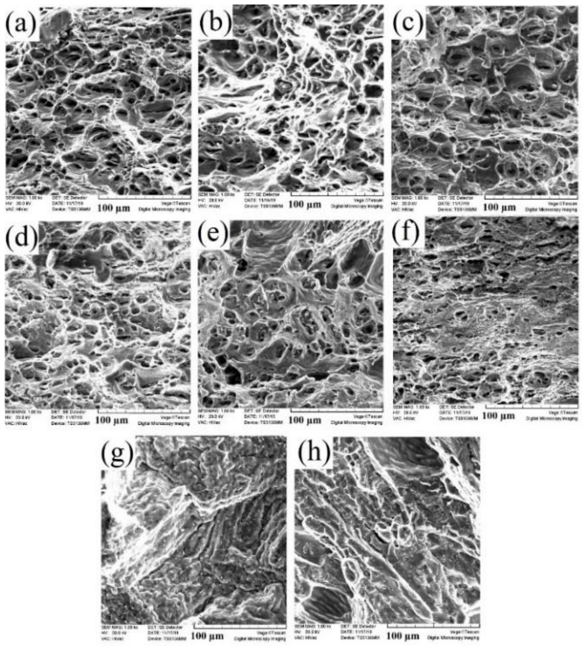

Figure 9. SEM micrographs of fracture surfaces for tensile tested (a) raw material (b) flux-free welded specimen (c) 2.5% SiO2 active flux welded specimen, (d) 7.5% SiO2active flux welded specimen, (e) 10% SiO2active flux welded specimen, (f) 2.5% TiO_2 active flux welded specimen, (g) 7.5% TiO_2 active flux welded specimen, (h) 10% TiO_2 active flux welded specimens

from ductile to brittle. If one looks at the Figures 9h and 9g, 7.5% and 10% TiO_2 active flux welded specimens, the fracture surfaces are completely flat showing that the fracture nature has become brittle. Moreover, some cracks are also observed in the fracture surfaces of 7.5% and 10% TiO_2 active flux welded specimens. The characteristics of both regions were quasi-cleavage with some secondary cracks.

4. CONCLUSIONS

This research was carried in order to increase the penetration depth and improve the mechanical properties of weld region by addition of the active fluxes of TiO_2 and SiO_2. Therefore, the effect of these active fluxes was investigated on microstructure properties of aluminum 6061 welded by TIG method. The following conclusions were obtained based on experimental results:

1) The stiffness and hardness of the base metal are increased due to the work-hardening occurred by creating a cast-like structure during welding. Therefore, the highest strength was related to the base metal. However, the strength of the base metal is also reduced by the loss of work hardening during the welding process.

2) The addition of active flux increased granularity in the weld zone leading to increase of tensile strength and

microhardness. Moreover, they decreased the grain size and increased the strength.

3) The highest tensile strength in SiO_2 added specimens was occurred in 10% SiO_2 added specimen with the amount of 138 MPa. The ratio of tensile strength in 10% SiO_2 added specimen to welded specimen without using flux was72%.

4) The highest tensile strength in TiO_2 added specimen was occurred in 10% TiO_2 added specimen with the amount of 152 MPa. The ratio of tensile strength in 10% TiO_2 added specimen to the specimen without using flux was 90%.

5) The effect of addition of TiO_2 flux was more considerable than that of SiO_2, because the TiO_2 had more nucleation effect than the SiO_2.

5. REFERENCES

1. Choudhary, S., Choudhary, S., Vaish, S., Upadhyay, A. K., Singla, A. and Singh, Y., "Effect of Welding Parameters on Microstructure and Mechanical Properties of Friction Stir Welded Al 6061 Aluminum Alloy Joints", ***Materials Today: Proceedings***, Vol. 25, No. 4, (2020), 563-569. doi: 10.1016/j.matpr.2019.05.466
2. Ahmad Fauzi, M. N., Uday M. B., Zuhailawati, H. and Ismail, A. B., "Microstructure and Mechanical Properties of Alumina-6061 Aluminum Alloy Joined by Friction Welding", ***Materials & Design***, Vol. 31, No. 2, (2010), 670-676. doi: 10.1016/j.matdes.2009.08.019
3. Wang, W., Fan, D., Huang, J. and Huang, Y., "Numerical Simulation of Arc Plasma and Weld Pool in Double Electrodes Tungsten Inert Gas Welding", ***International Journal of Heat and Mass Transfer***, Vol. 85, (2015), 924-934. doi: 10.1016/j.ijheatmasstransfer.2015.01.132
4. Singh, G., Kang, A. S., Singh, K. and Singh, J., "Experimental Comparison of Friction Stir Welding Process and TIG Welding Process for 6082-T6 Aluminum Alloy", ***Materials Today: Proceedings***, Vol. 4, No. 2, (2017), 3590-3600. doi: 10.1016/j.matpr.2017.02.251
5. Mishra, D. and Dakkili, M., "Gas Tungsten and Shielded Metal Arc Welding of Stainless Steel 310 and 304 Grades over Single and Double 'V' Butt Joints", ***Materials Today: Proceedings***, Vol. 27, No. 2, (2020), 772-776. doi: 10.1016/j.matpr.2019.12.189
6. Dong, B., Cai, X., Ni, Z., Lin, S., Fan, C. and Yang, C., "Numerical Simulation of Arc Characteristics in Narrow Gap TIG Welding", ***International Journal of Mechanical Sciences***, Vol. 161-162, (2019), 105031. doi: 10.1016/j.ijmecsci.2019.105031
7. Liu, Z., Fang, Y., Cui, S., Yi, S., Qiu, J., Jiang, Q., Liu, W. and Luo, Z., "Keyhole Thermal Behavior in GTAW Welding Process", ***International Journal of Thermal Sciences***, Vol. 114 (2017), 352-362. DOI: 10.1016/j.ijthermalsci.2017.01.005
8. Kulkarni, A., Dwivedi, D. K. and Vasudevan, M., "Study of Mechanism, Microstructure and Mechanical Properties of Activated Flux TIG Welded P91 Steel-P22 Steel Dissimilar Metal Joint", ***Materials Science and Engineering: A***, Vol. 731, (2018), 309-323. doi: 10.1016/j.msea.2018.06.054
9. Ramkumar, K. D., Chandrasekhar, A., Singh, A. K., Ahuja, S., Agarwal, A., Arivazhagan, N. and Rabel, A. M., "Comparative Studies on the Weldability, Microstructure and Tensile Properties of Autogeneous TIG Welded AISI 430 Ferritic Stainless Steel with and without Flux", ***Journal of Manufacturing Processes***, Vol. 20, No. 1, (2015), 54-69. doi: 10.1016/j.jmapro.2015.09.008
10. Venukumar, S., Sarkar, P., Sashank, J. S., Sampath, P. and Saikiran, K., "Microstructural and Mechanical Properties of Inconel 718 TIG Weldments", ***Materials Today: Proceedings***, Vol. 5, No. 2, (2018), 8480-8485. doi: 10.1016/j.matpr.2017.11.544
11. Ramkumar, K. D., Ramanand, R., Ameer, A., Simon, K. A. and Arivazhagan, N., "Effect of Post Weld Heat Treatment on the Microstructure and Tensile Properties of Activated Flux TIG Welds of Inconel X750", ***Materials Science and Engineering: A***, Vol. 658, (2016), 326-338. doi: 10.1016/j.msea.2016.02.022
12. Babbar, A., Kumar, A., Jain, V. and Gupta, D., "Enhancement of Activated Tungsten Inert Gas (A-TIG) Welding Using Multi-Component TiO_2-SiO_2-Al_2O_3 Hybrid Flux", ***Measurement***, Vol. 148, (2019), 106912. doi: 10.1016/j.measurement.2019.106912
13. Xie X., Shen, J., Cheng, L., Li, Y. and Pu, Y., "Effects of Nano-Particles Strengthening Activating Flux on the Microstructures and Mechanical Properties of TIG Welded AZ31 Magnesium Alloy Joints", ***Materials & Design***, Vol. 81, (2015), 31-38. doi: 10.1016/j.matdes.2015.05.024
14. Ezazi, M. A., Yusof, F., Sarhan, A. A. D., Shukor, M. H. A. and Fadzil, M., "Employment of Fiber Laser Technology to Weld Austenitic Stainless Steel 304l with Aluminum Alloy 5083 Using Pre-Placed Activating Flux", ***Materials & Design***, Vol. 87, (2015), 105-123. doi: 10.1016/j.matdes.2015.08.014
15. Khoshroyan, A. and Darvazi, A. R., "Effects of Welding Parameters and Welding Sequence on Residual Stress and Distortion in Al6061-T6 Aluminum Alloy for T-Shaped Welded Joint", ***Transactions of Nonferrous Metals Society of china***, Vol. 30, No. 1, (2020), 76-89. DOI: 10.1016/j.matdes.2015.08.014
16. Pk, J., Mc, G., Sharma, S., Shetty, R., Shettar, M. and Hiremath, P., "Influence of Homogenization and Aging on Tensile Strength and Fracture Behavior of TIG Welded Al6061-Sic Composites", ***Journal of Materials Research and Technology***, Vol. 9, No. 3, (2020), 3598-3613. doi: 10.1016/j.jmrt.2020.01.098
17. Surendran, N., Luhar, K., Mistry, D., Teacher, M. and Srivastav, S., "Effect of TiO_2 Flux and SiO_2 Flux Coating on Weld Penetration by A-TIG", ***SSRG International Journal of Mechanical Engineering***, Vol. 4, No. 4, (2018), 14-21. doi: 10.14445/23488360/IJME-V5I4P104
18. Li, C., Shi, Y., Gu, Y., Fan, D. and Zhu, M., "Effects of Different Activating Fluxes on the Surface Tension of Moltenmetal in Gas Tungsten Arc Welding", ***Journal of Manufacturing Processes***, Vol. 32, (2018), 395-402. doi: 10.1016/j.jmapro.2018.03.001
19. Morisada, Y., Fujii, H. and Xukun, W., "Development of Simplified Active Fluxtungsten Inert Gas Welding for Deep Penetration", ***Materials & Design***, Vol. 54, (2014), 526-530. DOI: 10.1016/j.matdes.2013.08.081
20. Savitskii, M., "The Mechanism of the Effects of Electrically-Negative Elements on the Penetrating Power of an Arc with a Tungsten Cathode", ***Avt. Svarka***, Vol. 9, (1980), 17-22.
21. Heiple, C. R. and Poper, J. R., "Mechanism for Minor Element Effect on GTA Fusion Zone Geometry***", Welding Journal***, Vol. 61, (1982), 975-1025.
22. Aruri, D., Adepu, K., Adepu, K. and Bazavada, K., "Wear and Mechanical Properties of 6061-T6 Aluminum Alloy Surface Hybrid Composites [(Sic+Gr) And (Sic+Al_2O_3)] Fabricated by Friction Stir Processing", ***Journal of Materials Research and Technology***, Vol. 2, No. 4, (2013), 362-369. doi: 10.1016/j.jmrt.2013.10.004
23. Sanket Bodkhe, D. R. D., "Effects of Flux Coated Tungsten Inert Gas Welding on 304L Austenitic Stainless Steel", ***IACSIT International Journal of Engineering and Technology***, Vol. 6, No. 3, (2014), 177-181. doi: 10.7763/IJET.2014.V6.691
24. JIS, J., "2201, Test pieces for tensile test for metallic material" Japanese Standards Association, (1998).

25. Zhang, T., Shen, J., LÜ, L., Wang, C., J.X. Sang, J. X. and D. Wu, D., "Effects of Graphene Nanoplates on Microstructures and Mechanical Properties of NSA-TIG Welded AZ31 Magnesium Alloy Joints", ***Transactions of Nonferrous Metals Society of China***, Vol. 27, (2017), 1285-1293. doi: 10.1016/s1003-6326(17)60149-3

26. Satputaley, S. S., Waware, Y., Ksheersagar, K., Jichkar, Y. and Khonde, K., "Experimental Investigation on Effect of TIG Welding Process on Chromoly 4130 And Aluminum 7075-T6", ***Materials Today: Proceedings***, Vol. 41, No. 5, (2021), 991-994. doi: 10.1016/j.matpr.2020.05.733

27. Zaretsky, E. B., N. Frage, N. and Kalabukhov, S., "Shock Wave Determination of the Strengthening of Commercial Aluminum Alloy 6061 by Point Defects", ***Materials Science and Engineering: A***, Vol. 761, (2019), 138066. doi: 10.1016/j.msea.2019.138066

28. Verma, J. and Taiwade, R. V., "Effect of Welding Processes and Conditions on the Microstructure, Mechanical Properties and Corrosion Resistance of Duplex Stainless-Steel Weldments-A Review", ***Journal of Manufacturing Processes***, Vol. 25, (2017), 134-152. doi: 10.1016/j.jmapro.2016.11.003

29. Ajezi-Sardroud, R., Mostafapour, A., Ajezi-Sardroud, F. and Mohtadi-Bonab, M.A., "Effect of activating flux on aluminum 6061 and its mechanical properties by gas tungsten arc welding process", ***International Journal of Engineering***, ***Transactions B: Applications,*** Vol. 35, No. 8, (2022), doi: 10.5829/IJE.2022.35.08B.06.

30. Jayakrishnan, S. and Chakravarthy, P., "Flux Bounded Tungsten Inert Gas Welding for Enhanced Weld Performance-A Review", ***Journal of Manufacturing Processes***, Vol. 28, No. 1, (2017), 116-130. doi: 10.1016/j.jmapro.2017.05.023

31. Li, C., Shi, Y., Gu, Y., Fan, D. and Zhu, M., "Effects of Different Activating Fluxes on the Surface Tension of Molten Metal in Gas Tungsten Arc Welding", ***Journal of Manufacturing Processes***, Vol. 32, (2018), 395-402. doi: 10.1016/j.jmapro.2018.03.001

32. Kulkarni, A. Dwivedi, D. K. and Vasudevan, M., "Effect of Oxide Fluxes on Activated TIG Welding of AISI 316l Austenitic Stainless Steel", ***Materials Today: Proceedings***, Vol. 18, (2019), 4695-4702. doi: 10.1016/j.matpr.2019.07.455

33. Xu, W. and Dávila, L. P., "Tensile Nanomechanics and the Hall-Petch Effect in Nanocrystalline Aluminum", ***Materials Science and Engineering: A***, Vol. 710, (2018), 413-418. doi: 10.1016/j.msea.2017.10.021

Persian Abstract

چکیده

تحقیق حاضر با هدف افزایش عمق نفوذ و بهبود خواص مکانیکی ناحیه جوش با افزودن فلاکس های فعال اکسید تیتانیوم و اکسید سیلیکون انجام یافت. جوشکاری گاز بی اثر تنگستن روی آلیاژ آلومینیوم ۶۰۶۱ اعمال شد و فلاکس های فعال اکسید تینانیوم و اکسید سیلیکون با ۲.۵، ۷.۵ و ۱۰ درصد وزنی اضافه شد. تاکنون جوشکاری گاز بی اثر تنگستن روی آلومینیوم ۶۰۶۱ با فلاکس های فعال اکسید تینانیوم و اکید سیلیکون انجام نشده است. در این تحقیق، خواص مکانیکی با استفاده از آزمایشات کششی و میکروسختی ویکرز تعیین شد. نتایج نشان می دهد که بیشترین مقاومت کششی مربوط به فلز پایه و در نمونه های جوش داده شده مربوط به فلاکس فعال اکسید تیتانیوم ۱۰درصد است. نسبت استحکام کششی با استفاده از فلاکس فعال تیتانیوم و بدون فلاکس ۹۰ درصد است. استفاده از هر دو فلاکس اکسید تیتانیوم فعال و اکسید سیلیکون، نمونه جوش داده شده را دانه بندی کرده و استحکام آن را افزایش می دهد. اثر افزودن فلاکس اکسید تیتانیوم بیشتر از فلاکس اکسید سیلیکون است زیرا اکسید تیتانیوم نقش کلیدی در دانه بندی نسبت به اکسید سیلیکون دارد.